Modulation of Drug Transport Properties by Multicomponent Diffusion in Surfactant Aqueous Solutions

Huixiang Zhang[†,‡] and Onofrio Annunziata*[,†]

Department of Chemistry, Texas Christian University, Fort Worth, Texas 76129, and Alcon Research, Ltd., Fort Worth, Texas 76134

Received May 27, 2008. Revised Manuscript Received July 1, 2008

Diffusion coefficients of drug compounds are crucial parameters used for modeling transport processes. Interestingly, diffusion of a solute can be generated not only by its own concentration gradient but also by concentration gradients of other solutes. This phenomenon is known as multicomponent diffusion. A multicomponent diffusion study on drug−surfactant−water ternary mixtures is reported here. Specifically, high-precision Rayleigh interferometry was used to determine multicomponent diffusion coefficients for the hydrocortisone−tyloxapol−water system at 25 °C. For comparison, diffusion measurements by dynamic light scattering were also performed. In addition, drug solubility was measured as a function of tyloxapol concentration, and drug−surfactant thermodynamic interactions using the two-phase partitioning model were characterized. The diffusion results are in agreement with a proposed coupled multicomponent diffusion model for ternary mixtures relevant to nonionic drug and surfactant molecules. Theoretical examination of diffusion-based drug transport in the presence of concentration gradients of micelles shows that drug fluxes and drug concentration profiles are significantly affected by coupled multicomponent diffusion. This work provides guidance for the development of accurate models of diffusion-based controlled release in multicomponent systems and for the applications of micelle concentration gradients to the modulation of diffusion-based drug transport.

Introduction

Diffusion occurs in a large number of biological, medical, laboratory, and manufacturing processes. Examples include controlled release of chemicals from their matrices, centrifugation, dialysis, crystallization, and mixing inside microfluidics. In the pharmaceutical industry, diffusion coefficients of drug compounds are crucial parameters used for modeling, predicting, and designing drug release and other transport processes.[1−5]

Interestingly, diffusion-based transport of a solute can be generated not only by its own concentration gradient but also by concentration gradients of other solutes in the mixture. This phenomenon is known as coupled multicomponent diffusion.[6−8] Since drug formulations typically include other additives besides the solvent, drug transport is expected to depend on the additive concentration gradients. Multicomponent diffusion is also expected to occur in gels (or other porous materials) permeated by these liquid mixtures, provided that corrections related to gel volume fraction and obstruction effect are taken into account.[9] Understanding multicomponent diffusion for these systems is not only important for accurate modeling of drug-transport processes such as diffusion-based controlled release, but also for predicting and designing novel configurations, where concentration-gradients of additives may be used to modulate the rate of drug diffusion.

Among all additives, surfactants are widely used in drug delivery to enhance drug aqueous solubility by micelle binding, reduce drug toxicity, facilitate control of drug uptake, and improve bioavailability of drugs.[10] In the presence of micelles, the self-diffusion coefficient of drug molecules is a weighted average of the self-diffusion coefficients of the free drug and the drug-micelle aggregates.[11−13] Since micelle diffusion is typically much slower than that of free drug molecules, surfactants impart a substantial effect on diffusion-based drug transport. Indeed, it has been shown that the addition of micelle in gels is a valuable tool for the modulation of drug-release rate.[14,15] However, drug transport is not only affected by association to micelles but also by micelle concentration gradients due to multicomponent diffusion effects.

Although there are several reports on binary and ternary diffusion in surfactant aqueous mixtures,[16−23] to our knowledge,

* To whom correspondence should be addressed: Department of Chemistry, Box 298860, Texas Christian University, Fort Worth, Texas 76129. Phone: (817) 257-6215. Fax: (817) 257-5851. E-mail: O.Annunziata@tcu.edu.

† Texas Christian University.

‡ Alcon Research, Ltd.

(1) Cussler, E. L. *Diffusion: Mass Transfer in Fluid Systems*; Cambridge University Press: Cambridge, U.K., 1997.

(2) Crank, J. *The Mathematics of Diffusion*; Oxford at the Clarendon Press: Oxford, 1956.

(3) Liang, S.; Xu, J.; Weng, L.; Dai, H.; Zhang, X.; Zhang, L. *J. Controlled Release* **2006**, *115*, 189–196.

(4) Weigl, B. H.; Yager, P. *Science* **1999**, *283*, 346–347.

(5) Kanjickal, D. G.; Lopina, S. T. *Crit. Rev. Ther. Drug Carrier Syst.* **2004**, *21*, 345–386.

(6) Taylor, R.; Krishna, R. *Multicomponent Mass Transfer*; John Wiley & Sons: New York, 1993.

(7) Tyrrell, H. J. V.; Harris, K. R. *Diffusion in Liquids*; Butterworths: London, 1984.

(8) Albright, J. G.; Annunziata, O.; Miller, D. G.; Paduano, L.; Pearlstein, A. J. *J. Am. Chem. Soc.* **1999**, *121*, 3256–3266.

(9) Lauffer, M. A. *Biophys. J.* **1961**, *1*, 205–213.

(10) Malmsten, M. *Surfactants and Polymers in Drug Delivery*; Marcel Dekker: New York, 2002.

(11) Soderman, O.; Stilbs, P.; Price, W. S. *Concepts Magn. Reson.* **2004**, *23A*, 121–135.

(12) Stilbs, P. *J. Colloid Interface Sci.* **1982**, *87*, 385–394.

(13) Momot, K. I.; Kuchel, P. W.; Chapman, B. E.; Deo, P.; Whittaker, D. *Langmuir* **2003**, *19*, 2088–2095.

(14) Paulsson, M.; Edsman, K. *J. Pharm. Sci.* **2001**, *90*, 1216–1225.

(15) Bramer, T.; Dew, N.; Edsman, K. *J. Pharm. Sci.* **2006**, *95*, 769–780.

(16) Weinhemer, R. M.; Evans, D. F.; Cussler, E. L. *J. Colloid Interface Sci.* **1981**, *80*, 357–368.

(17) Leaist, D. G. *J. Colloid Interface Sci.* **1986**, *111*, 230–239.

(18) Halvorsen, H. C.; Leaist, D. G. *Phys. Chem. Chem. Phys.* **2004**, *6*, 3515–3523.

(19) Leaist, D. G.; MacEwan, K. *J. Phys. Chem. B* **2001**, *105*, 690–695.

(20) D'Errico, G.; Ortona, O.; Paduano, L.; Vitagliano, V. *J. Colloid Interface Sci.* **2001**, *239*, 264–271.

(21) Castaldi, M.; Constatino, L.; Ortona, O.; Paduano, L.; Vitagliano, V. *Langmuir* **1998**, *14*, 5994–5998.

(22) Annunziata, O.; D'Errico, G.; Ortona, O.; Paduano, L.; Vitagliano, V. *J. Colloid Interface Sci.* **1999**, *216*, 8–15.

(23) Corti, M.; Degiorgio, V. *J. Phys. Chem.* **1981**, *85*, 711–717.

10.1021/la801636u CCC: $40.75
Published on Web 08/22/2008

there is no report on multicomponent diffusion for surfactant aqueous mixtures in the presence of drug molecules. It is important to observe that, although pulsed-gradient spin−echo NMR (PGSE-NMR) has been used to determine drug self-diffusion coefficients (or intradiffusion coefficients[7]), this technique does not provide interdiffusion coefficients.[7,11−13] Dynamic light scattering on the other hand has been extensively used to determine interdiffusion coefficients of micelles.[23] However, this technique is not sensitive to low-molecular-weight molecules and does not provide the appropriate coefficients needed to describe multicomponent diffusion in the presence of concentration gradients.[24,25] High-precision Rayleigh and Gouy interferometry,[26] and Taylor dispersion[27] are the most employed techniques for the determination of multicomponent diffusion coefficients. In relation to the solubilization process, two multicomponent diffusion studies by Taylor dispersion have been reported on ternary aqueous solutions of *n*-alcohols and sodium dodecylsulfate.[28,29] However, the theoretical interpretation of these systems is particularly difficult because of the anionic nature of the surfactant, its relatively high critical micelle concentration (cmc), and changes in size and shape of micelles.[29] Moreover, the molar concentrations of the *n*-alcohols employed in these experiments are significantly higher than those typical of drugs with relatively low solubility.

In this paper, a multicomponent diffusion study on drug−surfactant−water ternary mixtures is reported. Specifically, high-precision Rayleigh interferometry was used to determine multicomponent diffusion coefficients for the hydrocortisone−tyloxapol−water system at 25 °C. Hydrocortisone (11β,17α,21-trihydroxypregn-4-ene-3,20-dione) is a nonionic drug molecule mainly used in the treatment of inflammation and allergies.[30] Tyloxapol is a nonionic surfactant mostly used in marketed ophthalmic products and as a mucolytic agent for treating pulmonary diseases.[31−34] This surfactant is essentially an oligomer of the much investigated octoxynol 9 (Triton X-100). Since tyloxapol is made of monomeric units chemically bonded to each other, its cmc is much lower than that of the corresponding monomeric surfactant for entropic reasons.[31] Indeed, the concentration of free tyloxapol molecules can be neglected within our experimental concentration domain. Drug solubility as a function of tyloxapol concentration was also measured. We have used these data to determine drug−surfactant thermodynamic interactions using the well-established two-phase partitioning model.[12] The diffusion results are examined by reporting a novel multicomponent diffusion model for ternary mixtures relevant to nonionic drug and surfactant molecules. This model was used to theoretically examine fundamental aspects of diffusion-based drug transport in the presence of surfactant concentration gradients.

Although micelle formation and phase diagrams of the tyloxapol−water system have been reported, diffusion coefficients for the tyloxapol−water system are still missing. Hence, interferomentric diffusion measurements for this binary system were included in the paper. In addition, diffusion-coefficient measurements by dynamic light scattering were performed for comparison.

Theory

Ternary Diffusion. In the case the drug−surfactant−water ternary system, interdiffusion is described by the extended Fick's first law:[7,8]

$$-J_1 = D_{11}\nabla C_1 + D_{12}\nabla C_2 \tag{1a}$$

$$-J_2 = D_{21}\nabla C_1 + D_{22}\nabla C_2 \tag{1b}$$

Here, J_1 and J_2 are the molar fluxes of drug (1) and surfactant (2), respectively, and the four D_{ij}'s (with $i,j = 1,2$) are the ternary diffusion coefficients. Main-diffusion coefficients, D_{11} and D_{22}, describe the flux of a solute due to its own concentration gradient, while cross-diffusion coefficients, D_{12} and D_{21}, are responsible for the flux of a solute due to the concentration gradient of the other solute.

The interdiffusion coefficients in eqs 1a and 1b can be described relative to different reference frames.[35] In the volume-fixed frame, the fluxes of the components of a ternary system satisfy $(J_0)_V\bar{V}_0 + (J_1)_V\bar{V}_1 + (J_2)_V\bar{V}_2 = 0$; in the solvent-fixed frame, we have $(J_0)_0 = 0$. Here, J_i and $\bar{V}_i$ are the molar flux and partial molar volume of component i, respectively. The subscript "V" denotes the volume-fixed frame. The subscript "0" denotes the solvent component when appended directly to a flux, and denotes the solvent-fixed frame when appended outside the parentheses to an already-subscripted flux or diffusion coefficient. Since concentration differences are small and volume changes on mixing are negligible, our diffusion measurements correspond, to an excellent approximation, to the volume-fixed frame.[35]

The relation of diffusion to thermodynamics is simpler in the solvent-fixed frame.[36−38] Here, the fluxes for a ternary system can be written as

$$\begin{aligned}-(J_1)_0 &= (D_{11})_0\nabla C_1 + (D_{12})_0\nabla C_2\\ &= (L_{11})_0\nabla\mu_1 + (L_{12})_0\nabla\mu_2\end{aligned} \tag{2a}$$

$$\begin{aligned}-(J_2)_0 &= (D_{21})_0\nabla C_1 + (D_{22})_0\nabla C_2\\ &= (L_{21})_0\nabla\mu_1 + (L_{22})_0\nabla\mu_2\end{aligned} \tag{2b}$$

where $\mu_i$is the chemical potential of the ith component, and $(L_{ij})_0$ are the solvent-frame Onsager transport coefficients. These coefficients satisfy the Onsager reciprocal relation (ORR): $(L_{12})_0 = (L_{21})_0$.[39,40] We can use eqs 2a and 2b to relate the solvent-fixed diffusion coefficients and Onsager transport coefficients according to

$$(D_{11})_0 = (L_{11})_0\mu_{11} + (L_{12})_0\mu_{21} \tag{3a}$$

$$(D_{12})_0 = (L_{11})_0\mu_{12} + (L_{12})_0\mu_{22} \tag{3b}$$

$$(D_{21})_0 = (L_{21})_0\mu_{11} + (L_{22})_0\mu_{21} \tag{3c}$$

$$(D_{22})_0 = (L_{21})_0\mu_{12} + (L_{22})_0\mu_{22} \tag{3d}$$

(24) Leaist, D. G.; Hao, L. *J. Phys. Chem.* **1993**, *97*, 7763–7768.
(25) Annunziata, O.; Buzatu, D.; Albright, J. G. *Langmuir* **2005**, *21*, 12085–12089.
(26) Miller, D. G.; Albright; J. G. In *Measurement of the Transport Properties of Fluids: Experimental Thermodynamics*; Wakeham, W. A., Nagashima, A., Sengers, J. V., Eds.; Blackwell Scientific Publications: Oxford, 1991; Vol. *3*, pp 272−294.
(27) Leaist, D. G. *J. Phys. Chem.* **1990**, *94*, 5180–5183.
(28) Leaist, D. G. *Can. J. Chem.* **1990**, *68*, 33–35.
(29) Leaist, D. G.; Hao, L. *J. Chem. Soc., Faraday Trans.* **1995**, *91*, 2837–2842.
(30) Zor, U.; Her, E.; Talmon, J.; Moshonov, S. *Ann. N. Y. Acad. Sci.* **1988**, *524*, 456–457.
(31) Scott, H. *J. Colloid Interface Sci.* **1998**, *205*, 496–502.
(32) Regev, O.; Zana, R. *J. Colloid Interface Sci.* **1999**, *210*, 8–17.
(33) Westesen, K. *Int. J. Pharm.* **1994**, *102*, 91–100.
(34) Westesen, K.; Koch, M. H. J. *Int. J. Pharm.* **1994**, *103*, 225–236.
(35) Kirkwood, J. G.; Baldwin, R. L.; Dunlop, P. J.; Gosting, L. J.; Kegeles, G. *J. Chem. Phys.* **1960**, *33*, 1505–1513.
(36) Miller, D. G.; Vitagliano, V.; Sartorio, R. *J. Phys. Chem.* **1986**, *90*, 1509–1519.
(37) Dunlop, P. J.; Gosting, L. J. *J. Phys. Chem.* **1959**, *63*, 86–93.
(38) Woolf, L. A.; Miller, D. G.; Gosting, L. J. *J. Am. Chem. Soc.* **1962**, *84*, 317–331.
(39) Onsager, L. *Phys. Rev.* **1931**, *38*, 2265–2279.
(40) Miller, D. G. *J. Phys. Chem.* **1959**, *63*, 570–578.

where $\mu_{ij} \equiv (\partial\mu_i/\partial C_j)_{T,p,C_{k\neq j}}$, T is the temperature, and p is the pressure.[36−40] Furthermore, the chemical-potential derivatives obey the relation[40]

$$\mu_{12}(1 - C_2\bar{V}_2) - \mu_{11}C_1\bar{V}_2 = \mu_{21}(1 - C_1\bar{V}_1) - \mu_{22}C_2\bar{V}_1 \quad (4)$$

The volume-fixed frame coefficients, $(D_{ij})_V$, can be then related to the solvent-fixed frame coefficients $(D_{ij})_0$ using the following relations:[36,37]

$$(D_{11})_V = (1 - C_1\bar{V}_1)(D_{11})_0 - C_1\bar{V}_2(D_{21})_0 \quad (5a)$$

$$(D_{12})_V = (1 - C_1\bar{V}_1)(D_{12})_0 - C_1\bar{V}_2(D_{22})_0 \quad (5b)$$

$$(D_{21})_V = (1 - C_2\bar{V}_2)(D_{21})_0 - C_2\bar{V}_1(D_{11})_0 \quad (5c)$$

$$(D_{22})_V = (1 - C_2\bar{V}_2)(D_{22})_0 - C_2\bar{V}_1(D_{12})_0 \quad (5d)$$

Two-Phase Model. We consider a drug−surfactant−water ternary system at constant temperature. All system components are neutral. The composition of this system is characterized by the drug molar concentration, C_1, and surfactant molar concentration, C_2. We assume that the cmc is low compared to the experimental domain of surfactant concentrations. This implies that the surfactant in solution is essentially present as micelles only. Micelles are assumed to be monodisperse with aggregation number, m.

Solubilization of drug molecules into micelles can be described using the following chemical-equilibrium scheme:

$$\mathrm{M} + \mathrm{D} \rightleftharpoons \mathrm{MD}$$
$$\mathrm{MD} + \mathrm{D} \rightleftharpoons \mathrm{MD}_2$$
$$\cdots$$
$$\mathrm{MD}_{i-1} + \mathrm{D} \rightleftharpoons \mathrm{MD}_i$$
$$\cdots$$

where D denotes the free drug molecule in aqueous solution, M is the micelle and MD_i is the micelle−drug complex containing i drug molecules. Concentrations of individual species are related to the component concentrations through the following mass balances:

$$C_1 = C_D + \sum_{i=1} iC_{MD_i} \quad (6a)$$

$$C_2/m = C_M + \sum_{i=1} C_{MD_i} \quad (6b)$$

where C_D, C_M, and C_{MD_i} are the molar concentrations of drug, micelle, and drug−micelle complexes, respectively. The thermodynamic characterization of the drug−micelle interaction requires the measurements of a set of equilibrium constants. Since their experimental determination is not feasible, drug solubilization can be described employing a two-phase partitioning model.[12,29] Within this model, drug molecules are assumed to partition between the micelle-free aqueous pseudophase (free drug) and the micellar pseudophase (bound drug). This partitioning equilibrium is described by the following condition:

$$K = \frac{C_D^{(M)}}{C_D^{(W)}} = \frac{C_1 - C_D}{C_D}\frac{1 - \phi}{\phi} \quad (7)$$

where K is the partitioning constant, $C_D^{(M)}$and $C_D^{(W)}$ are the drug molar concentrations in the micellar and water pseudophases respectively, C_D is the free drug molar concentration in the total volume, and $\phi = C_2\bar{V}_2$ is the volume fraction of the micellar pseudophase. Equation 7 assumes ideal-dilute behavior with respect to the drug component.

The partitioning constant, K, can be determined from the dependence of drug solubility, S_1, on ϕ. The measured value of K can be then used to calculate C_D using eq 7. In the presence of chemical equilibrium between the aqueous pseudophase and the drug solid phase, $C_D^{(W)}$ is a constant independent of ϕ. Furthermore, $C_D^{(W)}$ is also the drug solubility, S_1^0, in pure water. In the presence of micelles, S_1 becomes the sum of two contributions: $C_D = S_1^0(1 - \phi)$ (free drug) and $C_D^{(M)}\phi = K S_1^0\phi$ (bound drug). Thus, drug solubility is described by the following linear relation:

$$S_1 = S_1^0[1 + (K - 1)\phi] \quad (8)$$

The average number of drug molecules per micelle defined by $\langle i\rangle \equiv \sum_{i=1} iC_{MD_i}/(C_2/m)$ can be also related to K. Using eq 6a and eq 7, we obtain

$$\langle i\rangle = \frac{C_1 - C_D}{(C_2/m)} = \frac{C_1}{(C_2/m)}\frac{K\phi}{1 - \phi + K\phi} \quad (9)$$

However, C_M and C_{MD_i} are not directly related to K. Their determination requires knowledge of the distribution function, $f(i)$, since $C_{MD_i} = f(i)\,(C_2/m)$. However, if drug−micelle binding is independent of i, it can assume that $f(i)$ is given by the Poisson distribution $(e^{-\langle i\rangle}/i!)\langle i\rangle^i$.[41] For this special case, the determination of C_M and C_{MD_i} requires only eq 9, which is based on the two-phase model.

Diffusion Model. The expressions for the thermodynamic factors, μ_{ij}, and the Onsager coefficients, $(L_{ij})_0$, in eqs 3a, 3b, 3c, and 3d can be derived using the two-phase partitioning model. To obtain expressions for the four thermodynamic factors, the following chemical-potential expressions are hypothesized:

$$\mu_1 = \mu_1^0 + RT \ln C_D^{(W)} \quad (10a)$$

$$m\mu_2 = m\mu_2^0 + RT \ln C_M + RT \ln y(\phi) \quad (10b)$$

where μ_1^0 and μ_2^0 are the standard chemical potentials, and R is the ideal-gas constant. Equation 10a is consistent with the two-phase partitioning model and can be used to derive eq 7. On the other hand, eq10b is an addition to the two-phase model and characterizes the translational entropy of the micelles, which is the driving force for their diffusion. The micelle activity coefficient, $y(\phi)$, describes the deviation from ideal-dilute solution and is assumed to be independent of drug concentration. Equations 10a and 10b can be rewritten as

$$(\mu_1 - \mu_1^0)/RT = \ln C_1 - \ln[1 + (K - 1)\phi] \quad (11a)$$

$$(\mu_2 - \mu_2^0)/RT = \frac{1}{m}\ln\frac{y(\phi)C_2}{m} - \frac{C_1}{C_2}\frac{K\phi}{1 - \phi + K\phi} \quad (11b)$$

where we have used eqs 7−9. Expressions for the thermodynamic factors are obtained by differentiation:

$$C_1(\mu_{11}/RT) = 1 \quad (12a)$$

$$C_2(\mu_{12}/RT) = -\frac{(K - 1)\phi}{1 - \phi + K\phi} \quad (12b)$$

$$C_2(\mu_{21}/RT) = -\frac{K\phi}{1 - \phi + K\phi} \quad (12c)$$

$$C_2(\mu_{22}/RT) = \frac{\beta}{m} + \frac{K(K - 1)\phi^2}{(1 - \phi + K\phi)^2}\frac{C_1}{C_2} \quad (12d)$$

where $\beta \equiv 1 + (\mathrm{d} \ln y/\mathrm{d} \ln C_2)$ is the thermodynamic factor of the binary surfactant−water system, and $\beta = 1$ in the limit of low surfactant concentrations. It is important to observe that eqs 12a, 12b, 12c, and 12d become consistent with eq 4 if $\bar{V}_1 = 0$.

This is a limitation of the two-phase partitioning model, which assumes that drug molecules do not affect the volume of both pseudophases. This approximation is reasonable for solutions dilute in drug.

Expressions for the Onsager coefficients can be obtained by assuming that the solvent-frame fluxes of individual species in solution are uncoupled, and the micelle diffusion coefficient does not depend on drug binding:

$$-J_D = C_D D_D \nabla \mu_D / RT \tag{13a}$$

$$-J_M = C_M D_M \nabla \mu_M / RT \tag{13b}$$

$$-J_{MD_i} = C_{MD_i} D_M \nabla \mu_{MD_i} / RT \qquad \text{with } i = 1, 2, ... \tag{13c}$$

where D_D and D_M are the mobilities of free drug and micelle, respectively. In eqs 13a, 13b, and 13c, J_D, J_M, and J_{MD_i} are the solvent-frame fluxes of the individual species, and μ_D, μ_M, and μ_{MD_i} are the corresponding chemical potentials. Fluxes of individual species are related to the component fluxes through the following mass balances:

$$(J_1)_0 = J_D + \sum_{i=1} i J_{MD_i} \tag{14a}$$

$$(J_2)_0/m = J_M + \sum_{i=1} J_{MD_i} \tag{14b}$$

while, since $\mu_1 = \mu_D$ and $m\mu_2 = \mu_M$, the following chemical-potential relations are obtained:

$$\nabla \mu_D = \nabla \mu_1 \tag{15a}$$

$$\nabla \mu_M = m \nabla \mu_2 \tag{15b}$$

$$\nabla \mu_{MD_i} = i \nabla \mu_1 + m \nabla \mu_2 \qquad \text{with } i = 1, 2, ... \tag{15c}$$

Equations 13−15 lead to the following flux expressions for the components:

$$-(J_1)_0 = \left(C_D D_D + D_M \sum_{i=1} i^2 C_{MD_i}\right) \frac{\nabla \mu_1}{RT} + m D_M \sum_{i=1} i C_{MD_i} \frac{\nabla \mu_2}{RT} \tag{16a}$$

$$-(J_2)_0 = m D_M \sum_{i=1} i C_{MD_i} \frac{\nabla \mu_1}{RT} + m^2 D_M \left(C_M + \sum_{i=1} C_{MD_i}\right) \frac{\nabla \mu_2}{RT} \tag{16b}$$

where the ORR is respected. Comparison between eqs 2a and 2b and eqs 16a and 16b yields:

$$RT(L_{11})_0 = C_D D_D + \langle i^2 \rangle (C_2/m) D_M \tag{17a}$$

$$RT(L_{12})_0 = RT(L_{21})_0 = \langle i \rangle C_2 D_M \tag{17b}$$

$$RT(L_{22})_0 = m C_2 D_M \tag{17c}$$

where $\langle i^2 \rangle \equiv \sum_{i=1} i^2 C_{MD_i}/(C_2/m)$, and $\langle i^2 \rangle = \langle i \rangle + \langle i \rangle^2$ for the Poisson distribution. Equations 3, 5, 15, and 20 can be used to obtain $(D_{ij})_0$ and $(D_{ij})_V$:

$$(D_{11})_V = (D_{11})_0 = \frac{(1-\phi) D_D + K\phi D_M}{1 - \phi + K\phi} \tag{18a}$$

$$(D_{12})_V = (D_{12})_0 - C_1(\phi/C_2)(D_{22})_0 = -\frac{C_1(\phi/C_2)(K-1)(1-\phi)(D_D - \kappa D_M)}{(1 - \phi + K\phi)^2} \tag{18b}$$

$$(D_{21})_V = (1-\phi)(D_{21})_0 = 0 \tag{18c}$$

$$(D_{22})_V = (1-\phi)(D_{22})_0 = (1-\phi)\beta D_M \tag{18d}$$

where $\kappa \equiv [\beta + (\beta - 1)K\phi - 2\beta\phi - \beta(K-1)\phi^2]/(1-\phi)$ and $\bar{V}_1 = 0$ consistently with the two-phase model. Note that $\beta \approx 1$ and $\kappa \approx 1$ when the surfactant volume fraction is small.

The drug main-diffusion coefficient, $(D_{11})_V$ is independent of C_1 and represents the average $w\, D_D + (1-w)\, D_M$, where $w = (\partial C_D/\partial C_1)_{C_2}$ from eq 7. Since $(\partial C_D/\partial C_1)_{C_2} = C_D/C_1$, $(D_{11})_V$ coincides with the drug self-diffusion coefficient.[12] Note that $(D_{11})_V$ decreases as the surfactant concentration increases because $D_M < D_D$. The drug cross-diffusion coefficient, $(D_{12})_V$, is negative because $K > 1$ and $D_D > \kappa D_M$ in eq 18b, and approaches zero if $C_1 = 0$. The condition $K > 1$ is a direct consequence of drug solubility being enhanced in the presence of micelles (see eq 8). Furthermore, since $\kappa \approx 1$ and $D_D > \kappa D_M$, $D_D - \kappa D_M \approx D_D - D_M$ is a reasonable approximation. The surfactant main-diffusion coefficient, $(D_{22})_V$, in eq 18d is given by the corresponding expression for the binary surfactant−water system. This is expected because the drug component has no effect on the thermodynamic and transport properties of the micelles according to the two-phase model. For the same reason, $(D_{21})_V$ can be neglected according to eq 18c. In conclusion, the most significant result of the diffusion model is represented by the expressions for the drug diffusion coefficients, $(D_{11})_V$ and $(D_{12})_V$. It is important to observe that the conditions $K \gg 1$ and $\phi \ll 1$ often apply to poorly soluble drugs in surfactant aqueous formulations. Hence, eqs 18a and 18b can be approximated by

$$(D_{11})_V = \frac{D_D + K\phi D_M}{1 + K\phi} \tag{19a}$$

$$(D_{12})_V = -\frac{C_1 \bar{V}_2 K (D_D - D_M)}{(1 + K\phi)^2} \tag{19b}$$

Equations 19a and 19b will be used to describe our experimental data and to examine the role of multicomponent diffusion on diffusion-based drug transport.

Materials and Methods

Materials. Hydrocortisone (purity >98%) was purchased from Sigma (Sigma Chemical Co., St. Louis, MO) and used without further purification. Dexamethasone (purity 100%) and rimexolone (purity 98%) were kindly donated by Alcon Research, Ltd. and used without further purification. Tyloxapol (SigmaUltra grade) was purchased from Sigma and used without further purification. The molecular weights for hydrocortisone, dexamethasone, rimexolone and tyloxapol were taken to be 362.47 g mol^{-1}, 392.46 g mol^{-1}, 370.25 g mol^{-1}, and 4500 g mol^{-1} respectively. Deionized water was passed through a four-stage Millipore filter system to provide high purity water for all the experiments. Stock solutions of tyloxapol−water and hydrocortisone−tyloxapol−water were made by weight with an error of about 0.1% in their concentrations. Precise masses of stock solutions were added to flasks and diluted with pure water to reach the final target concentrations of the solutions used for the diffusion experiments. High-performance liquid chromatography (HPLC)-grade phosphoric acid and acetonitrile were purchased from EMD Chemicals, Inc. (Gibbstown, NJ).

Density Measurements. Molar concentrations of the solutions were obtained from density. All density measurements were made with a Mettler-Paar DMA40 density meter, thermostatted with water from a large, well-regulated (±1 mK) water bath.

Solubility Measurements. Solid drug compound (hydrocortisone, dexamethasone, or rimexolone) was added in excess to tyloxapol−water solutions in glass vials. The obtained heterogeneous samples were continuously agitated for 7 days in a regulated water bath at 25.0 ± 0.1 °C. Aliquots of the suspensions were then passed through 0.2-μm filters (Millipore) and, if necessary, diluted with the HLPC mobile phase (see below) so that the final drug concentration was

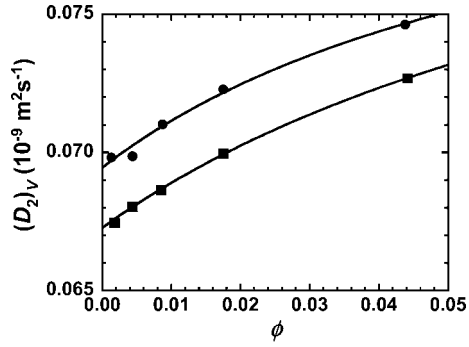

Figure 1. Diffusion coefficients for the binary tyloxapol−water system as a function of tyloxapol volume fraction measured by Rayleigh inteferometry (circles) and dynamic light scattering (squares) at 25 °C. The solid curves are quadratic fits through the data.

around 0.1 g/L. The drug concentration of the properly diluted samples was then measured using HPLC (Waters Alliance 2695) with a UV detector (Waters model 2487). For hydrocortisone and dexamethasone assay, a Waters Symmetry C18 column (size: 3.9 × 150 mm) was employed with a mobile phase consisting of a 73/27 (v/v) mixture of 0.3% aqueous phosphate buffer (pH 3)/acetonitrile with a flow rate of 1.5 mL/min. Chromatograms were obtained at 254 nm. For rimexolone assay, a Phenomenex Spherisorb ODS(2) column (size: 4.6 × 250 mm) was employed with a mobile phase consisting of 40/60 (v/v) water/acetonitrile with a flow rate of 1.0 mL/min. Chromatograms were obtained at 242 nm.

Rayleigh Interferometry. Diffusion measurements on ternary hydrocortisone−tyloxapol−water systems and corresponding binary aqueous systems were made with a high-precision Gosting diffusiometer operated in its Rayleigh interferometric optical mode.[7,26] A comprehensive description of the Gosting diffusiometer can be found in ref 8 and references therein. Details on individual diffusion measurements and a description of the method are reported as Supporting Information.

Dynamic Light Scattering. Diffusion measurements by dynamic light scattering were performed at 25.0 ± 0.1 °C on tyloxapol−water binary solutions. All samples were filtered through a 0.02-μm filter (Anotop 10, Whatman). The experiments were performed on a light scattering apparatus built using the following main components: He−Ne laser (35 mW, 632.8 nm, Coherent Radiation), manual goniometer and thermostat (Photocor Instruments), multitau correlator, and APD detector and software (PD4042, Precision Detectors). All experiments were performed at the scattering angle $\theta = 90°$. The scattering vector $q = (4\pi n/\lambda)\sin(\theta/2)$ was calculated using $n = 1.33$ and $\lambda = 632.8$ nm.

Results

Diffusion in the Tyloxapol−Water System. Measurements of inter diffusion coefficients, $(D_2)_V$, were performed on the tyloxapol−water binary system at 25 °C by both Rayleigh interferometry and dynamic light scattering. The results are shown in Figure 1. Surfactant volume fractions were obtained using $\phi = C_2\bar{V}_2$, where $\bar{V}_2 = 3.98$ L mol^{-1} is the tyloxapol partial molar volume. This quantity, which was calculated from density measurements, was found to be independent of concentration within the experimental error up to concentrations as high as 10%. The tyloxapol−water system has a cmc of 0.038_5 g/L at 25 °C.[31] This concentration, which corresponds to a volume fraction of $\phi = 3.4 \times 10^{-5}$, is significantly smaller than the surfactant concentrations employed in our experiments. Thus, it can be assumed that all tyloxapol is present in micellar form.

As shown in Figure 1, $(D_2)_V$ increases with ϕ in both cases. However, the light-scattering values were found to be 3% lower than the corresponding interferometric values. This systematic small discrepancy is expected because of the effect of tyloxapol small polydispersity and theoretical differences between the two methods.[25,42] To quantitatively examine our diffusion results, our data are fitted within the linear range (with $\phi < 0.02$) using the equation $(D_2)_V = D_M(1 + \alpha\phi)$. The values $D_M = (0.0694 \pm 0.0002)\ 10^{-9}$ m^2 s^{-1} and $\alpha = 2.3 \pm 0.3$ from the interferometric measurements, and $D_M = (0.0673 \pm 0.0001)\ 10^{-9}$ m^2 s^{-1} and $\alpha = 2.3 \pm 0.1$ from the light-scattering measurements were obtained. The two values of α, which coincide within the experimental error, are consistent with the presence of net repulsive interactions between the micelles.[23] Note that tyloxapol micelles are spherical, and their size and shape do not change significantly for concentration as high as 10% by weight according to cryo-transmission electron microscopy.[32] Light-scattering measurements were found to be more reproducible than the corresponding interferometric measurements at the two lowest surfactant concentrations ($\phi \leq 0.005$). In these conditions, dynamic light scattering remains a very sensitive technique as a result of the large molecular weight of the micelles. Nonetheless, the accuracy of the Rayleigh interferometric method is expected to be higher because of its simpler relation to diffusion coefficients and polydispersity, and better experimental setup. Hence, the D_M values extracted from interferometric measurements are expected to be more accurate. This value was used to calculate the micelle hydrodynamic radius, R_h, through the Stokes−Einstein equation.[1] The value of $R_h = 3.53$ nm was obtained, which is in excellent agreement with previously reported small-angle X-ray scattering measurements.[32] The corresponding hydrodynamic volume, $V_h = 111$ L mol^{-1}, can be used to estimate the micelle aggregation number. Since tyloxapol consists of ~7 octyl-phenol-ethoxylate monomers with ~10 ethoxy groups each, and there are about four water molecules associated with each ethoxy group,[43] it can be estimated that ~280 water molecules are bound to each tyloxapol molecule. Since the molar volumes of tyloxapol and water are 3.98 L mol^{-1} and 0.018 L mol^{-1}, respectively, each hydrated tyloxapol occupies ~9 dm^3 mol^{-1}. This leads to an aggregation number of $m \approx 12$ per tyloxapol molecule, which corresponds to ~90 octyl-phenol-ethoxylate monomers inside one micelle. This value is consistent with the aggregation number, $m \approx 100$, of the octyl-phenol-ethoxylate surfactant (Triton X-100).[44]

Drug Solubility in Tyloxapol−Water Solutions. In Figure 2, the solubility data for hydrocortisone, dexamethasone, and rimexolone are shown as a function of tyloxapol volume fraction at 25 °C. These three drug compounds have significantly different solubility in water. This has allowed us to describe the range of K values typical of drug compounds. In all cases, drug solubility, S_1, linearly increases with ϕ. To quantitatively examine our solubility results, our data were fitted using eq 8. The obtained values of drug solubility in water, S_1^0, and partitioning constant, K, are listed in the figure caption. As expected, the affinity toward the micelle, which is represented by the values of K, correlates with S_1^0.

Diffusion in the Hydrocortisone−Tyloxapol−Water System. Interferometric measurements of multicomponent diffusion coefficients, $(D_{ij})_V$, on the hydrocortisone(1)−tyloxapol(2)−water ternary system were performed at 25 °C. The results are reported in Table 1. Ternary diffusion measurements on drug−surfactant−water systems could be performed only in the hydrocortisone case because of the very low aqueous solubility of dexamethasone and rimexolone. Indeed, the refractive-index contribution of the

(41) Feller, W. *An Introduction to Probability Theory and Its Applications*, 2nd ed.; John Wiley & Sons: New York, 1957; Vol. *1*.
(42) Zhang, H.; Annunziata, O. *J. Phys. Chem. B* **2008**, *112*, 3633–3643.
(43) Nilsson, P. G.; Lindman, B. *J. Phys. Chem.* **1983**, *87*, 4756–4761.
(44) Tummino, P. J.; Gafni, A. *Biophys. J.* **1993**, *64*, 1580–1587.

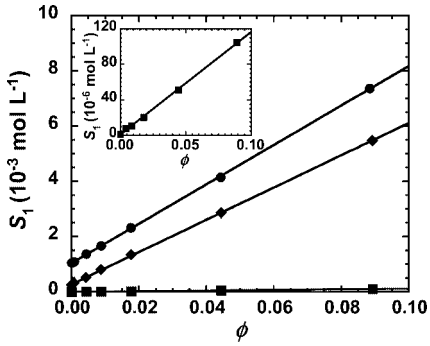

Figure 2. Solubility of hydrocortisone (circles), dexamethasone (diamonds) and rimexolone (squares) in tyloxapol−water mixtures as a function of tyloxapol volume fraction at 25 °C. The solid curves are linear fits through the data using eq 8. The obtained values of S_1^0/mM are 1.02 ± 0.01, 0.27 ± 0.01, and 0.0012 ± 0.0006 for hydrocortisone, dexamethasone, and rimexolone, respectively. The corresponding values of partitioning constant, K, are 70 ± 1, 220 ± 10, and 1000 ± 500. The inset shows a magnified view of rimexolone solubility data.

drug component cannot be precisely determined (dexamethasone) or even detected (rimexolone).

The drug main-diffusion coefficient, $(D_{11})_V$, decreases as the surfactant concentration increases as predicted by eq 19a. Correspondingly, the surfactant main-diffusion coefficient, $(D_{22})_V$, coincides with the binary, $(D_2)_V$, within the experimental error. The $(D_{11})_V$ and $(D_{22})_V$ values are plotted in Figure 3 as a function of ϕ, assuming that changes in C_1 have a negligible effect on both diffusion coefficients. It is important to remark that the curve in Figure 3 associated with the $(D_{11})_V$ data was obtained using eq 19a with $D_D = 0.53\ 10^{-9}$ m^2 s^{-1}, $D_M = 0.0694\ 10^{-9}$ m^2 s^{-1}, and $K = 70$ (see Table 1). Thus, our experimental values of $(D_{11})_V$ are in very good agreement with eq 19a and our solubility data. Furthermore, our ternary $(D_{22})_V$ data essentially coincide with the corresponding binary values as expected from eq 18d.

The drug cross-diffusion coefficient, $(D_{12})_V$, in Table 1 is negative, as predicted by eq 19b. Since $(D_{12})_V$ is directly proportional to C_1, $(D_{12})_V/C_1$ is plotted in Figure 4. The corresponding curve represents $(D_{12})_V/C_1$ calculated using eq 19b with the same values of D_D, D_M, and K used for $(D_{11})_V$. As shown in this figure, our experimental values of $(D_{12})_V$ are consistent with eq 19b.

The values of the surfactant cross-diffusion coefficient, $(D_{21})_V$, in Table 1 display a large relative error. Only the value at the highest surfactant concentration allows us to conclude that $(D_{21})_V > 0$. Since $(D_{21})_V = 0$ at $C_2 = 0$, our results suggest that $(D_{21})_V$ increases with ϕ. The large relative error associated with this diffusion coefficient is related to the small number of fringes employed for the experiments with drug concentration gradients (see Supporting Information), and to the small value of $(D_{21})_V$ itself. On the latter issue, we can compare $(D_{21})_V$ with $(D_{12})_V$. A proper comparison can be made by considering the corresponding $|(D_{ij})_V/[(D_{ii})_V C_i]|$ quotients. In this case, it is found that $|(D_{21})_V/[(D_{22})_V C_2]|$ is at least 1 order of magnitude smaller than $|(D_{12})_V/[(D_{11})_V C_1]|$. That $(D_{21})_V$ is small is consistent with eq 18c. In conclusion, our diffusion model accurately describes our experimental ternary diffusion coefficients.

Discussion

The effect of cross-diffusion on diffusion-based drug transport in the presence of micelles is examined by considering the flux expression given by eq 1a in the volume frame of reference:

$$-(J_1)_V = (D_{11})_V \nabla C_1 + (D_{12})_V \nabla C_2 \qquad (20)$$

The predicted value of $(J_1)_V$ is compared with that obtained ignoring the cross-diffusion term: $(D_{12})_V \nabla C_2$. For simplicity, it is convenient to consider one-dimensional diffusion along the X axis. Using eqs 19a, 19b, and 20 and introducing dimensionless variables, we obtain

$$-\psi = \frac{1+\gamma\omega}{1+\omega}\frac{dz}{dx} - \frac{z(1-\gamma)}{(1+\omega)^2}\frac{d\omega}{dx} \qquad (21)$$

where $\psi \equiv (J_1)_V/(D_D C_1^0/h)$ and $z \equiv C_1/C_1^0$ are the reduced drug flux and concentration, respectively, $x \equiv X/h$, $\omega \equiv K\phi$, $\gamma \equiv D_M/D_D$ (with $0 < \gamma < 1$), and C_1^0 and h are characteristic drug concentration and length, respectively. Note that, although eqs 19a, 19b become accurate when $\phi \ll 1$ and $K \gg 1$, these limits introduce no restriction on the accessible values of ω. Equation 21 can be rewritten in the following compact form:

$$-\psi = \frac{d(gz)}{dx} \qquad (22)$$

where $g \equiv (1 + \gamma\omega)/(1 + \omega)$ with $0 < g < 1$. If the cross-diffusion term in eq 21 is ignored, we obtain

$$-\psi' = g\frac{dz}{dx} \qquad (23)$$

where ψ' is the reduced drug flux predicted in the absence of coupled diffusion. Equation 23 relates the drug flux directly to its self-diffusion coefficient $(D_{11})_V = g D_D$, and becomes equivalent to eq 22 in the limits of $\gamma = 1$ or ω constant.

To examine some fundamental aspects of multicomponent diffusion, we consider steady-state diffusion occurring between two compartments[6] separated by an intermediate section with length, h, representing either a capillary tube or a porous media (e.g., gel). The concentration of drug and surfactant inside the two compartments are uniform and constant in order to achieve steady-state conditions. The flux of micelles is given by $-(J_2)_V = (D_{22})_V \nabla C_2$, where $(D_{22})_V = D_M$ is assumed to be constant. Drug diffusion occurring through the intermediate section, is described by the reduced flux, ψ, and the corresponding profiles of reduced concentration, z. General expressions of fluxes and concentration profiles relevant to these boundary conditions are reported in the Appendix.

In Figure 5a,b,c, three cases of steady-state diffusion are shown. In Figure 5a (case A), drug and micelles are located inside the left compartment (L) with concentrations C_1^0 and C_2^0, respectively. Drug and micelle concentrations inside the right compartment (R) are zero. In Figure 5b (case B), drug and micelles are located inside L with concentrations C_1^0 and C_2^0, respectively, and the micelle concentration inside R is zero as in case A. However, the drug concentration inside R is also C_1^0. Finally, in Figure 5c (case C), drug is located inside L with concentration C_1^0, and micelles are located inside R with concentration C_2^0. In all cases, concentrations in L and R are described using dimensionless

Table 1. Diffusion Coefficients for the Ternary Hydrocortisone−Tyloxapol−Water System

C_1 (10^{-3} mol L^{-1})	0.37	0.60	0.75	1.20	1.60
C_2 (10^{-3} mol L^{-1})	0	1.10	2.19	4.40	11.0
$(D_{11})_V$ (10^{-9} m^2 s^{-1})	0.53 ± 0.01	0.46 ± 0.01	0.343 ± 0.002	0.274 ± 0.002	0.168 ± 0.001
$(D_{22})_V$ (10^{-9} m^2 s^{-1})		0.0698 ± 0.0004	0.0707 ± 0.0004	0.0719 ± 0.0004	0.0737 ± 0.0004
$(D_{12})_V$ (10^{-9} m^2 s^{-1})		−0.04 ± 0.01	−0.05 ± 0.02	−0.03 ± 0.01	−0.01 ± 0.01
$(D_{21})_V$ (10^{-9} m^2 s^{-1})	0	0.001 ± 0.001	−0.001 ± 0.001	0.001 ± 0.001	0.0012 ± 0.0005

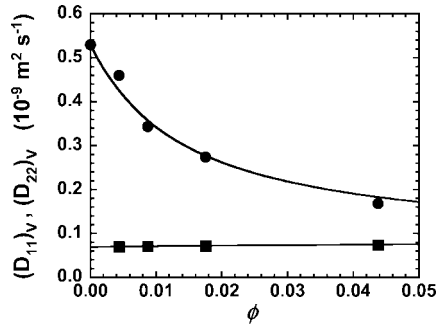

Figure 3. Hydrocortisone (circles) and tyloxapol (squares) main-diffusion coefficients, $(D_{11})_V$ and $(D_{22})_V$ as a function of tyloxapol volume fraction measured by Rayleigh inteferometry at 25 °C. The solid curves represent $(D_{11})_V$ calculated using eq 19a, and the $(D_2)_V$ binary curve shown in Figure 1.

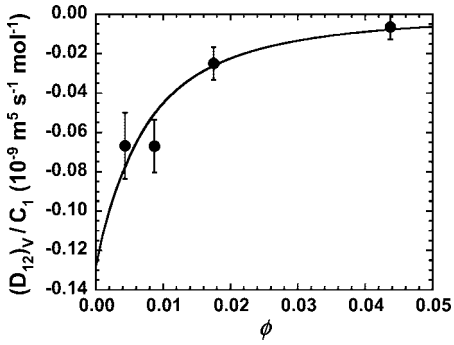

Figure 4. Ratio of hydrocortisone cross-diffusion coefficient, $(D_{12})_V$, to hydrocortisone concentration, C_1, as a function of tyloxapol volume fraction measured by Rayleigh inteferometry at 25 °C. The solid curve represents $(D_{12})_V/C_1$ calculated using eq 19b.

parameters: $z = 0$ or $z = 1$ for drug, and $\omega = 0$ or $\omega = \omega_0 \equiv K\bar{V}_2C_2^0$ for micelles. In Table 2, the corresponding expressions of reduced flux ψ and concentration profile z inside the intermediate section obtained using eqs A2 and A3 of the Appendix are reported.

For case A, the contribution of cross-diffusion is examined by taking the ratio ψ/ψ', where ψ' is obtained using eq A5. This ratio is plotted in Figure 6 as a function of ω_0 at several values of γ. Since $(D_{12})_V \leq 0$, cross-diffusion hinders drug transport from L to R away from the micelles. Hence, $\psi/\psi' \leq 1$. This effect vanishes in the limits of $\omega_0 \rightarrow 0$ and $\omega_0 \rightarrow \infty$, which correspond to the drug−water and micelle−water binary systems, respectively. In the latter case, all drug molecules are bound to the micelles. As shown in Figure 6, ψ/ψ' displays a minimum when reported as a function of ω_0 at a constant γ. The predicted minimum corresponds to the maximum contribution of cross-diffusion. In these conditions, $\psi/\psi' \approx 0.7$ when $\gamma \approx 0.1$ and $\psi/\psi' \approx 0.5-0.6$ when $\gamma \approx 0.01$. Thus, cross-diffusion significantly contributes to drug diffusion when micelle concentration is neither very low nor very high. In the case of our experimentally investigated systems, the surfactant volume fractions for which the contribution of cross-diffusion is the largest can be predicted. Since $\gamma = 0.13$ and $K = 70$ for the hydrocortisone case, cross-diffusion has maximum at $\omega_0 = 5.3$. This corresponds to the surfactant volume fraction of $\phi = 0.076$. For dexamethasone and rimexolone cases, it is reasonable to assume that $\gamma \approx 0.1$ as in the hydrocortisone case. This implies that that coupled diffusion is maximum at $\omega \approx 6$ and $\psi/\psi' \approx 0.7$. This yields $\phi \approx 0.03$ for dexamethasone ($K = 220$) and $\phi \approx 0.006$ for rimexolone ($K =$ 1000). The predicted volume fractions are typically employed in pharmaceutical and detergent formulations.

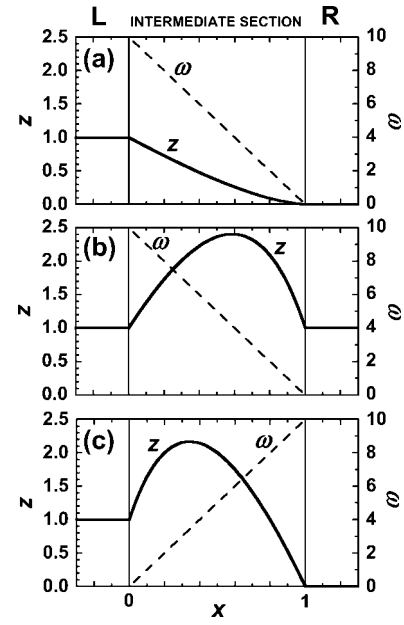

Figure 5. Schematic diagram of one-dimensional steady-state diffusion occurring between two compartments (L and R). The two solid vertical lines at $x = 0$ and $x = 1$ define the intermediate section, where diffusion occurs. The solid (z) and dashed (ω) curves describe the drug and surfactant concentration profiles. (a) Drug and micelle concentrations inside L are C_1^0 and C_2^0, respectively, while their concentrations inside R are both equal to zero. (b) Drug and micelle concentrations inside L are C_1^0 and C_2^0, respectively, while their concentrations inside R are C_1^0 and zero. (c) Drug and micelle concentrations inside L are C_1^0 and zero, respectively, while their concentrations inside R are zero and C_2^0. In each case, $\gamma = 0.1$ and $\omega_0 = 10$.

Table 2. Mathematical Expressions for Drug Fluxes and Concentration Profiles

case	ψ	z
A	$(1 + \gamma\omega_0)/(1 + \omega_0)$	$(\omega/\omega_0)[(1 + \gamma\omega_0)/(1 + \gamma\omega)]$ $[(1 + \omega)/(1 + \omega_0)]$
B	$(1 + \gamma\omega_0)/(1 + \omega_0) - 1$	$[(1 + \gamma\omega + \omega_0 - \omega)/(1 + \gamma\omega)]$ $[(1 + \omega)/(1 + \omega_0)]$
C	1	$[(\omega_0 - \omega)/\omega_0]$ $[(1 + \omega)/(1 + \gamma\omega)]$

For case B, drug diffusion is entirely related to cross-diffusion because $\psi' = 0$. Since $(D_{12})_V \leq 0$, there is a net drug flux from R to L driven by the micelle concentration gradient. The corresponding expression of ψ is reported in Table 2. Interestingly,

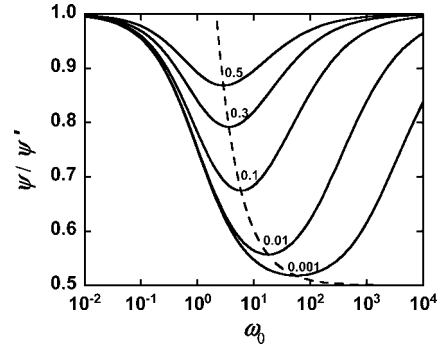

Figure 6. Ratio ψ/ψ' for case A as a function of ω_0 (solid curves) at several values of γ. The numbers associated with each solid curve identify the corresponding values of γ. The dashed curve represents the value of ω_0 at the minimum as a function of γ.

as shown in Figure 5b, the presence of maximum in the drug concentration profile due to cross-diffusion is predicted. According to the corresponding expression of z reported in Table 2, the maximum increases as ω_0 increases or γ decreases. The predicted behavior is related to the decrease of $|(D_{12})_V|$ as the micelle volume fraction, ϕ, increases (see eq 19b). As the drug enters into the intermediate section from R, $|(D_{12})_V|$ is the largest. However, $|(D_{12})_V|$ decreases from R to L due to the corresponding increase in ϕ. Since drug flux is constant, the drug concentration increases to produce compensating concentration gradients along the intermediate section. This example indicates that a gradient of micelle concentration can produce a significant increase of drug concentration in the gradient region.

If cross-diffusion were ignored, cases A and C would have been characterized by the same expression of ψ'. However, since $(D_{12})_V \leq 0$, cross-diffusion enhances drug diffusion from L to R, toward the micelles. Indeed, $\psi = 1$ (see Table 2) is predicted, as in the case of $\phi = 0$. This result implies that cross-diffusion compensates for the decrease of $(D_{11})_V$ occurring as the micelle volume fraction increases from L to R. As in case B, the presence of maximum in the z profile is shown in Figure 6c. The predicted behavior is related to the decrease of $|(D_{12})_V|$ as ϕ increases from L to R.

Conclusions

Multicomponent diffusion for a drug−surfactant−water system was experimentally and theoretically investigated. Fundamental aspects of cross-diffusion were discussed by examining three cases of drug diffusion in the presence of surfactant concentration gradients under steady-state conditions. Cross-diffusion significantly contributes to the diffusion-based transport of drug from a donating reservoir to a receiving reservoir for surfactant compositions typically employed in pharmaceutical and chemical industries. Furthermore, concentration gradients of surfactants can induce significant drug diffusion even if drug concentration is uniform. For this case, our model predicts that a gradient of surfactant concentration can produce significant increase of drug concentration in the gradient region. These aspects should be considered for the development of accurate models of diffusion-based controlled release in multicomponent systems and for the applications of surfactant concentration gradients to the modulation of diffusion-based drug transport.

Acknowledgment. The authors are indebted to Prof. John G. Albright for his assistance with the Gosting diffusiometer. This work was partially supported by TCU Research and Creative Activity Funds.

Appendix: General Solutions for One-Dimensional Steady-State Diffusion

We derive the general expressions for the fluxes, ψ and ψ', occurring between the two compartments (L and R) in steady-state conditions. The flux ψ can be obtained by integrating eq 22 from $x = 0$ to $x = 1$:

$$-\psi\int_0^1 \mathrm{d}x = \int_{g(\omega_L)z_L}^{g(\omega_R)z_R} \mathrm{d}gz \tag{A1}$$

where z_L and z_R are the values of z associated with L and R, respectively, while ω_L and ω_R are the corresponding values of ω. It is important to observe that the micelle concentration inside the intermediate section changes linearly with x since $(D_{22})_V = D_M$ constant and $(D_{21})_V = 0$. Thus, we can write $\omega = (1 - x)\,\omega_L + x\,\omega_R$. Using eq A1, the following flux expression is obtained:

$$\psi = \frac{1+\gamma\omega_L}{1+\omega_L}z_L - \frac{1+\gamma\omega_R}{1+\omega_R}z_R \tag{A2}$$

The corresponding drug concentration profile inside the intermediate section is obtained by integrating eq 22 from $x = 0$ to a generic x:

$$z = \frac{\dfrac{1+\gamma\omega_L}{1+\omega_L}z_L - \psi\dfrac{\omega-\omega_L}{\omega_R-\omega_L}}{\dfrac{1+\gamma\omega}{1+\omega}} \tag{A3}$$

The flux ψ' can be obtained by integrating eq 23 from $x = 0$ to $x = 1$:

$$-\psi'\int_0^1 \frac{\mathrm{d}x}{g} = \int_{z_L}^{z_R} \mathrm{d}z \tag{A4}$$

Using eq A4, the following flux expression is obtained:

$$\psi' = \frac{\gamma^2(\omega_R-\omega_L)}{\gamma(\omega_R-\omega_L) + (\gamma-1)\ln\dfrac{1+\gamma\omega_R}{1+\gamma\omega_L}}(z_L - z_R) \tag{A5}$$

where $\int[(1+\omega)/(1+\gamma\omega)]\,\mathrm{d}\omega = \gamma^{-1}\omega + \gamma^{-2}(\gamma-1)\ln(1+\gamma\omega)$ was applied.

The corresponding drug concentration profile inside the intermediate section is obtained by integrating eq 23 from $x = 0$ to a generic x:

$$z = z_L - \psi'\frac{\gamma(\omega-\omega_L) + (\gamma-1)\ln\dfrac{1+\gamma\omega}{1+\gamma\omega_L}}{\gamma^2(\omega_R-\omega_L)} \tag{A6}$$

Supporting Information Available: Interferometric diffusion data. This material is available free of charge via the Internet at http://pubs.acs.org.

LA801636U